Accurate Kinematic-Parameters Estimation Using IMU and GPS Sensors Fusion

S. Paul and T. K. Maiti, *Member, IEEE*

***Abstract*—In this work, we developed a kinematic parameters estimator (KPE) using Global Positioning System (GPS) and Inertial Measurement Unit (IMU) sensors embedded with a microcontroller. A Kalman filter is implemented in KPE to fuse IMU and GPS information. The filter estimates the short-range and long-rage positions simultaneously with the combination of the GPS data and IMU orientation information. We considered Kalman filter for sensor fusion which provides accurate position estimation despite of noise and drift. We have also performed the field trials to demonstrate the usability of the developed KPE. Evaluation of proposed solution through experiments in indoor and outdoor environments, demonstrating the position accuracy with few *cm* for short-range positioning and within a *meter* for long-range positioning.**

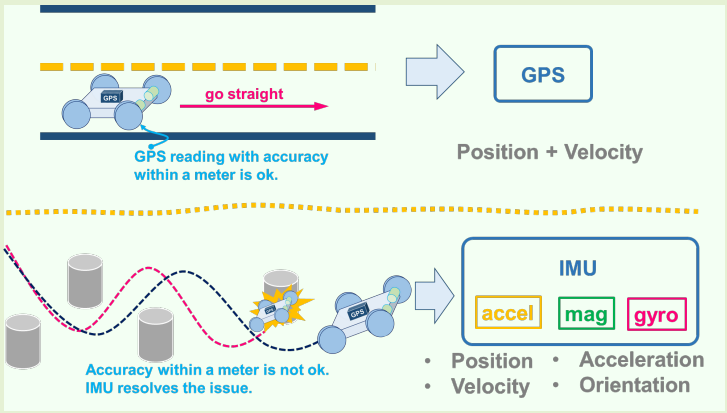

***Index Terms*—GPS, IMU, Kalman Filter, Kinematic Parameters, Sensor Fusion.**

I. Introduction

ONE of the essential constrain in a robot system is the estimating accurate kinematics parameters such as position, velocity, and acceleration in physical environments to control robot movements [1]-[5]. Numerous sensor devices such as GPS, camera, LiDAR (Light Detection and Ranging), IMU etc., were considered for position detection within accuracy less than a centimeter [6]-[17]. However, they all have certain limitations, for example, sensors like cameras and LiDAR cannot function appropriately in dark, dust, or foggy environments [11], [13]. In these scenarios, IMUs (Inertial Measurement Units) are used which consists an accelerometer, a gyroscope, and a magnetometer [8], [9], [12]. IMU is independent of the surroundings, used to detect the local position where accuracy less than a meter is not sufficient or needs the accuracy within few centimeters. Hellmers *et. al.*, reported an indoor positioning system that uses an IMU and magneto-inductive tracking technique to estimate the robot's position using a Kalman filter to achieve an accuracy of 0.44*m* in a 100*m* trajectory [18]. Poulose *et. al.*, developed an indoor position estimation algorithm in smartphone embedded with IMU sensor which estimates the robot position with an accuracy of 0.25*m* in a 40*m* trajectory [19]. Yao *et. al.*, proposed an integrated IMU and ultra-wideband (UWB) sensor-based indoor positioning system. They implemented a particle filter algorithm to estimate the robot position with an accuracy of 0.2*m* in a 50*m* trajectory [20]. Liu *et al.*, also developed an indoor localization system using smartphone inertial sensors [21]. They achieved an accuracy of 1.26*m* in a 150*m* trajectory which is more accurate than reported results in [18], [19], [20]. Accelerometers measure linear acceleration, gyroscopes measure angular velocity, and magnetometers measure the magnetic field. Combining these measurements makes estimating a moving robot kinematics parameters such as position, velocity, and orientation possible [1] [22].

GPS also gives a reasonable position estimation which is used in the scenarios where accuracy with in a meter is sufficient. It has certain drawbacks for ground robot localization such as requires a clear sky to function correctly and not a reliable option in case of indoor use [15]-[17]. Elsheikh *et al.*, proposed an integrated global navigation satellite system (GNSS) precise point positioning and reduced inertial sensor system for lane-level car navigation [15]. They used a tightly coupled integration method to combine the GNSS and inertial sensor measurements to an accuracy of 0.2*m* in a 500*m* trajectory. Abd Rabbou and El-Rabbany investigated the tightly coupled integration of GPS precise point positioning and MEMS-based inertial systems to an accuracy of 1.68*m* in a 20*km* trajectory [17]. Fastellini et al. demonstrate that integrating GNSS with IMU enhances positioning accuracy, crucial for precise road surveying as required by Italian law [28]. Ku et al., develops a motion capture system combining Differential Global Positioning Systems (DGPS) and MEMS IMUs for sub-millimetre

The work has been supported by The Gujarat Council on Science and Technology (GUJCOST), Department of Science & Technology, Government of Gujarat, India.

S. Paul is with the DA-IICT, Reliance Cross Rd, Gandhinagar, Gujarat, 382007 (e-mail: subhadeep_paul@daiict.ac.in).

T. K. Maiti is with the DA-IICT, Reliance Cross Rd, Gandhinagar, Gujarat, 382007 (e-mail: tapas_kumar@daiict.ac.in).

accuracy in animal locomotion studies [29], [30]. Zhang et al., propose a novel framework combining GPS/IMU data with vehicular-to-everything (V2X) networks to improve vehicular positioning accuracy in weak GPS signal conditions [31]. In another work, Zhang et al. use Variational Mode Decomposition–Improved Wavelet Denoising (VMD-IWD) and Temporal Dynamic Attention Neural Network (TDANN) to maintain inertial sensor-based systems (INS) /GPS navigation accuracy during GPS outages [32]. Zhang et al., also present a GNSS/IMU/Camera integrated system for comprehensive positioning in various scenarios [33]. Recently, Park et al., use the Iterative Closest Point (ICP) algorithm to align GPS and IMU data, improving indoor positioning accuracy for applications like factory navigation [34].

Most of the research group reported their work on only the position estimation [6]-[17]. Very few research group reported their results are either on velocity or acceleration estimations [1]-[5], [22] which are necessary for the accurate control of robot movements. This paper presents an accurate estimation of all three kinematics parameters such as position, velocity, and acceleration. In this paper, we present the implementation of a Kinematic Parameters Estimator (KPE) designed to integrate data from IMU and Global Positioning System (GPS) sensors using a Kalman filter for position estimation in GPS-denied environments. We have conducted experimental validations to assess the advantages and limitations of GPS-based global positioning and IMU-based local positioning systems. By fusing data from GPS and IMU sensors, our system addresses the challenges associated with each individual method. It effectively manages GPS outages and reduces errors inherent in IMU measurements, thereby providing a stable and highly accurate position in global coordinates (latitude and longitude). The system operates efficiently in real-time and ensures precise location detection when GPS signals are unavailable or compromised, such as in underpasses, tunnels, urban canyons, underground environments, and dense forests. The system's performance has been verified through multiple field trials and demonstrations. During these trials, we achieved centimeter-level accuracy for short-range positioning in the local frame and meter-level accuracy for long-range positioning in global coordinates.

The rest of the paper organized as follows: a kinematic-parameter estimators is developed using an IMU and GPS sensor fusion which is described in Section II. A Kalman filter is implemented in the estimator to fuse IMU and GPS measurements. The filter estimates the position by combining the GPS reading and the orientation information from the IMU. The implementation technique is described in Section III. We considered Kalman filter for sensor fusion which provides accurate estimation despite noise and drift. The results of the field trials have been evaluated and discussed in Section IV. Evaluation of proposed solution through experiments in indoor and outdoor environments, demonstrating accuracy and reliability. Several key insights and comparisons with previous works have been drawn and discussed.

II. Kinematic Parameter Estimator

To build the kinematic parameter estimator (KPE), we used BNO055 IMU and MTK3339 on Chip (SoC) GPS sensors, embedded with an ATmega328 microcontroller [23]-[25]. The BNO055 IMU is a 9-DOF (degree-of-freedom) sensor, acceleration ranges ±2g/±4g/±8g/±16g, outputs the quaternion, Euler angles, linear acceleration; operates between - 40°C to 85°C. MTK3339 on chip (SoC) GPS system has position accuracy of 1.8m, velocity accuracy of 0.1 m/s, and operating temperature ranges from -40°C to 85°C. The ATmega328 is a low-power, low-cost, high-performance AVR® RISC-based microcontroller integrated with 32KB Flash memory, 1KB EEPROM, 2KB SRAM, 23-GPIO (general-purpose input/output), serial programmable USART, SPI serial port, 6-channel 10-bit A/D converter, etc., and operates between 1.8V to 5.5V. The architectural flow diagram for interfacing BNO055 and MTK3339 with the ATmega328 microcontroller is shown in the Fig. 1. The BNO055 IMU measures acceleration and rotation, while the MTK3339 GPS

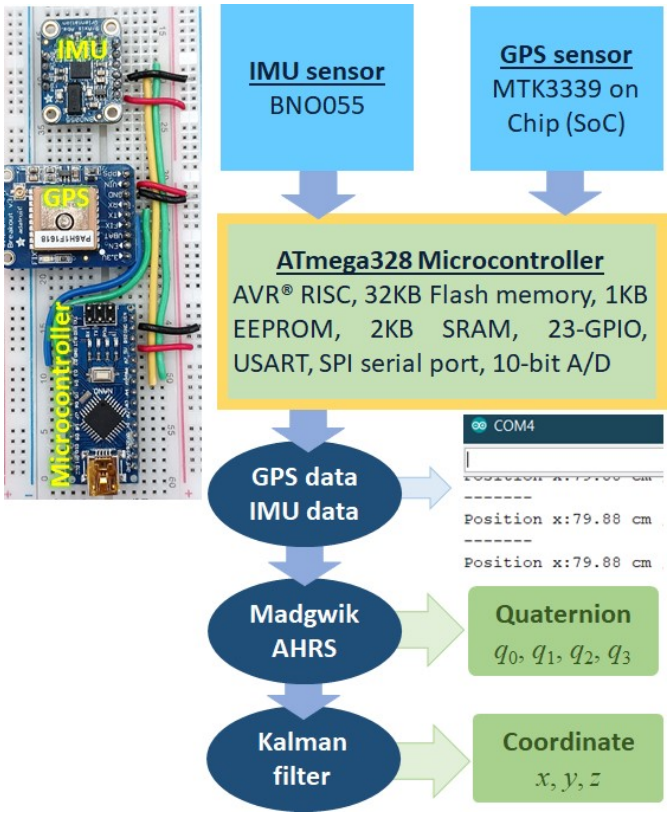

Fig. 1. The architectural flow diagram of the system, interfacing MTK3339 on Chip (SoC) GPS and BNO055 IMU sensors with the ATmega328 microcontroller, also IMU and GPS sensors data flow process through Madgwik and Kalman filter are schematically illustrated.

determines location and speed through satellite signals. The raw GPS and IMU data, i.e., latitude, longitude, altitude, pitch, yaw, roll, absolute north acceleration, absolute east acceleration, absolute up acceleration, velocity north, velocity east, velocity down, velocity error, altitude error are sent over the serial port from microcontroller.

We performed a series of experiments to validate our current localization system. At first, we started with distance

measurements using only IMU sensor within accuracy few centimeters in range and gives incorrect results in measurements of long distances. We found reasons for this inaccuracy: the acceleration values, obtained from IMU are highly sensitive, oriented along the axis of IMU, and not with a global axis or earth frame. To overcome this problem, we used angular velocity to find the orientation of the IMU which consists of build in accelerometers and gyro sensors [23]. These sensors work together to provide accurate measurements of an object's movement. Accelerometer measures acceleration a_x, a_y, and a_z in the x, y, and z directions, respectively as depicted in Fig. 2. Figure 3 shows angular velocity ω_x, ω_y, and ω_z around the x, y, and z axes, respectively obtained from gyroscope. One of the advantages of using an IMU is that it provides accurate measurements of an object's movement without requiring external references, such as GPS or landmarks. This makes it worthwhile when

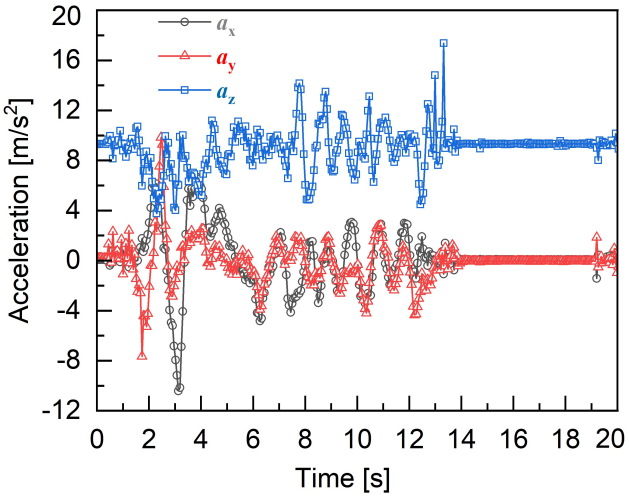

Fig. 2. Measured acceleration data a_x, a_y, and a_z along the x, y, and z, axis, respectively. The magnitude of a_z is higher than the a_x and a_y due to the effect of gravitational force on IMU sensor.

GPS signals are blocked or unavailable, such as underground

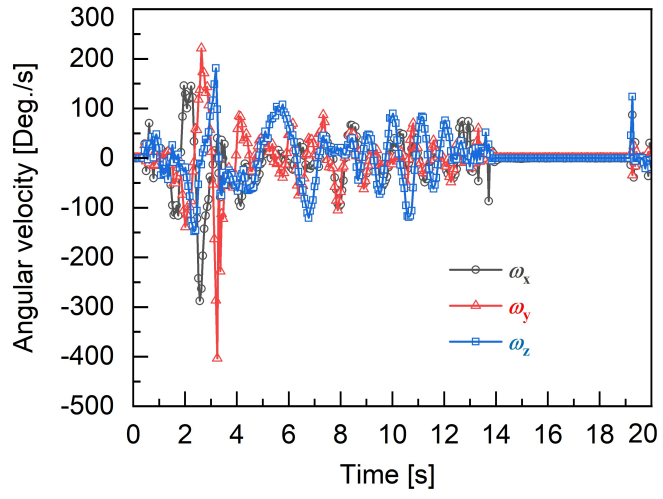

Fig. 3. Measured gyro-sensor data ω_x, ω_y, and ω_z. Here ω_x, ω_y, and ω_z are angular velocity along the x, y, and z, axis, respectively. Both acceleration components (shown in Fig. 2) and angular velocity components are fed to Kalman filter via Madgwik algorithm for accurate short-range position detection.

Fig. 4. Long-range outdoor position measured with GPS sensor (MTK3339 SoC) and mapped in Google Earth. Position accuracy within a meter is acceptable for outdoor application.

or indoors. GPS receivers provides accurate location information within a few meters, making it useful for navigation and mapping as illustrated in Fig. 4 with Google Earth map.

III. IMU AND GPS SENSORS FUSION

The GPS and IMU data obtained from the micro controller, processed using Kalman filter [5], [18], [26]. We considered the Kalman filter to fuse IMU and GPS data and measure the accurate position. This process helps to generate a detailed and accurate mapping of the path traveled by the object locally as well as globally. To implement the Kalman filter for sensor fusion in KPE, we used the following approach (1).

$$\left.\begin{matrix}\text{Accelerometer}\\ \text{Gyroscope}\end{matrix}\right\}\text{IMU} \rightarrow \begin{matrix}a_x,\ a_y,\ a_z\\ \omega_x,\ \omega_y,\ \omega_z\end{matrix} \rightarrow \frac{\text{Pitch,Yaw,Roll}}{a_{\text{NORTH}}, a_{\text{EAST}}, a_{\text{DOWN}}} \quad (1)$$

The equation 1 is the overview of the process of getting the earth frame acceleration from accelerometer and gyroscope data. This method has implemented in several steps. First, we obtained the acceleration components (a_x, a_y, a_z), and angular velocity components (ω_x, ω_y, ω_z) in all three directions x, y, and z, respectively, and then fed it to an AHRS (**A**ttitude and **H**eading **R**eference **S**ystems) algorithm. We used the Madgwik filter [27] as AHRS, which gives the quaternion as output. The quaternion is a mathematical construct representing rotations and orientations in three-dimensional space which has a four-component number system that extends the properties of complex numbers to three dimensions. We expressed quaternion as q_0, q_1, q_2, q_3 as presented in (2).

$$\begin{matrix}a_x,\ a_y,\ a_z\\ \omega_x,\ \omega_y,\ \omega_z\end{matrix} \rightarrow \underbrace{\begin{pmatrix}\text{Madgwik}\\ \text{Quaternion}\\ \text{update}\end{pmatrix}}_{\text{AHRS}} \rightarrow \underbrace{(q_0, q_1, q_2, q_3)}_{\text{Quaternion}} \quad (2)$$

The Madgwik AHRS uses the following equations to find the quaternion q_0, q_1, q_2, and q_3. The initial orientation is calibrated with assumptions,

$$\hat{q}_{est,t-1} = \begin{bmatrix} 1 \\ 0 \\ 0 \\ 0 \end{bmatrix}^T \quad \text{and} \quad v = \begin{bmatrix} 2\cdot(q_1\cdot q_3 - q_0\cdot q_2) \\ 2\cdot(q_0\cdot q_1 + q_2\cdot q_3) \\ 1-2\cdot(q_1^2+q_2^2) \end{bmatrix}^T \quad (3)$$

Here $q_{est,t-1}$ is the estimated q at time t-1. By using (3), the error in angular velocity, ω_{error} is calibrated using accelerometer reading as,

$$\omega_{error} = \begin{bmatrix} a_x & a_y & a_z \end{bmatrix} \times v \quad (4)$$

$$\omega = \begin{bmatrix} \omega_x & \omega_y & \omega_z \end{bmatrix} = \omega_{measured} + \omega_{error} \quad (5)$$

Then we found the angular velocity ω_t at time t as $\omega_t = [\omega_x\ \omega_y\ \omega_z]$. Change in quaternion value with Δt change in time is given by,

$$\dot{q}_{\omega,t} = \frac{1}{2}\cdot\hat{q}_{est,t-1} \otimes \omega_t \quad (6)$$

Therefore, we obtained the value of new quaternion as,

$$q_{\omega,t} = \hat{q}_{est,t-1} + \dot{q}_{\omega,t}\cdot\Delta t \quad (7)$$

Using the quaternion values of (7), we get end up with rotation matrix (8), implemented in kinematic parameter estimator (KPE),

$$R = \begin{bmatrix} 1-2(q_2^2+q_3^2) & 2(q_1\cdot q_2 - q_0\cdot q_3) & 2(q_0\cdot q_2 + q_1\cdot q_3) \\ 2(q_1\cdot q_2 + q_0\cdot q_3) & 1-2(q_1^2+q_3^2) & 2(q_2\cdot q_3 - q_0\cdot q_1) \\ 2(q_1\cdot q_3 - q_0\cdot q_2) & 2(q_0\cdot q_1 + q_2\cdot q_3) & 1-2(q_1^2+q_2^2) \end{bmatrix} \quad (8)$$

We used the rotation matrix to find the earth frame acceleration, i.e., acceleration in north (a_{NORTH}), east (a_{EAST}), and down (a_{DOWN}).

$$\begin{bmatrix} a_{NORTH} \\ a_{EAST} \\ a_{DOWN} \end{bmatrix} = R \times \begin{bmatrix} a_x \\ a_y \\ a_z \end{bmatrix} \quad (9)$$

We convert the acceleration data to the earth frame (North, East, Down) coordinate system using this orientation which is depicted in Fig. 5. A significant change with respect to the measured acceleration data (see Fig. 2) is highlighted with dotted circle (green) where the a_{NORTH}, a_{EAST}, and a_{DOWN} values represent along the earth global.

We used a first order low-pass (LF) Butterworth filter to overcome the sensitivity issue of accelerometers. The frequency response of an n^{th} order LF Butterworth filter is given as,

$$H(f) = \frac{A_m}{\sqrt{1+\varepsilon^2\left(f/f_c\right)^{2n}}} \quad (10)$$

Here n, f, f_c, and ε are the order of the filter, operating frequency (pass-band frequency), cut-off frequency, and maximum pass-band gain at A_m, = 1 respectively. These modifications successfully reduced the initial limitations to an extent which results the accuracy to a few meters of distance, is also not wildly fluctuating in a short time. Further experimentation and analysis show that long-term drift of the gyroscope creates the incorrect orientation value as output. This phenomenon results from the earth's rotation along its axis. To overcome this drift problem, we implemented a first order Butterworth high pass filter (HF). The frequency

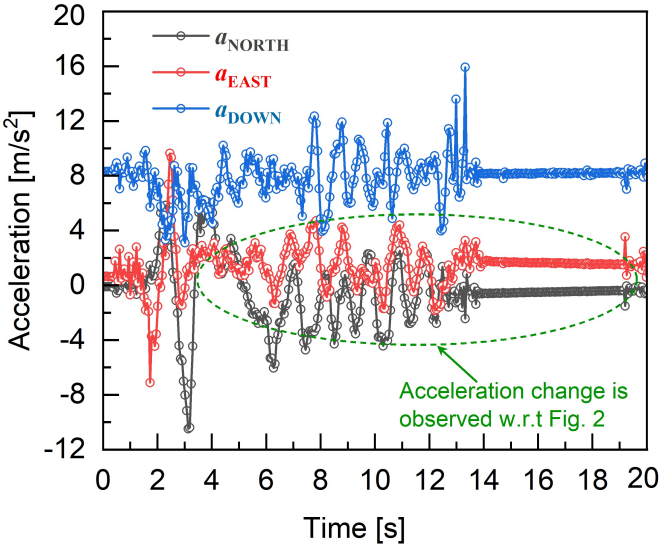

Fig. 5. Earth frame acceleration in north (a_{NORTH}), east (a_{EAST}), and down (a_{DOWN}) are obtained using Madgwik AHRS. Significant variation with respect to the measured data (shown in Fig. 2) is highlighted. These acceleration values represent along the earth global direction and irrespective of the KPE axis.

response of the filter is given by,

$$H(f) = \frac{A_m\left(f/f_L\right)}{\sqrt{1+\left(f/f_L\right)^2}} \quad (11)$$

Here A_m, f, and f_L are the maximum pass-band gain (A_m, = 1), operating frequency (pass-band frequency), and cut-off frequency, respectively. The HF and LF help reduce the drift and sensitivity problem of IMU and stabilize the measurements but cannot provide any global position. It measures the distance from its starting position and not from any globally indexed position. However, it does not give any absolute position of the KPE, always have to know about the initial position of the KPE. Although these results are obvious,

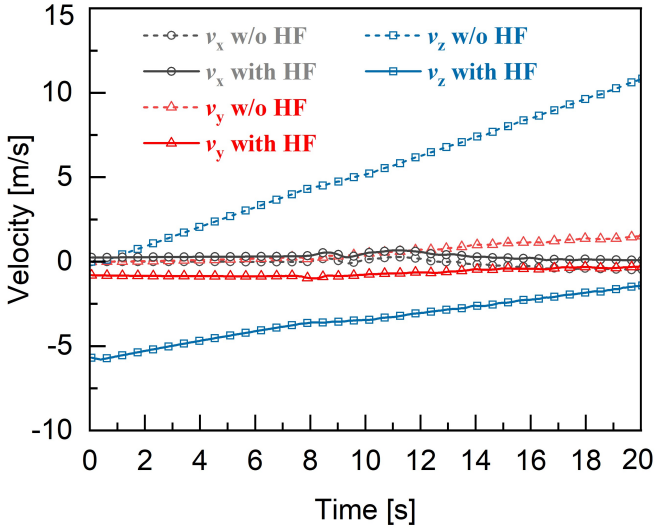

Fig.6. Compare the velocity components v_x, v_y, and v_z along x, y, and z directions, respectively with and without high-pass filter (HF). We observed that the slope of velocity components decreases for the use of HF which indicates the reduction of long-term drift effect in IMU sensor responses.

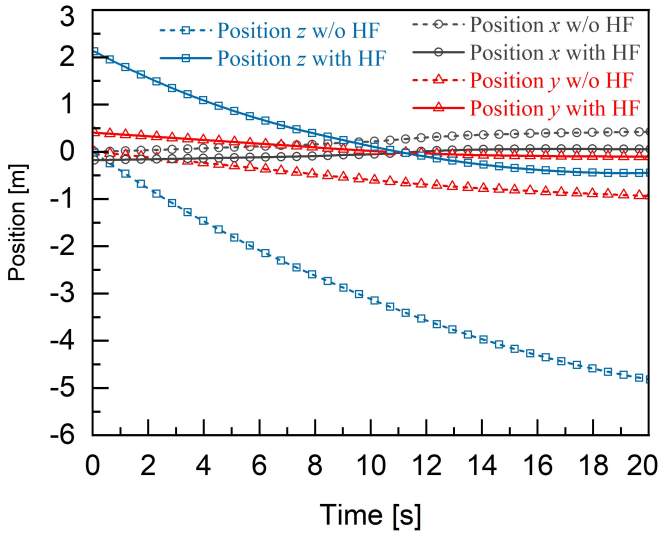

Fig. 7. Comparisons of position components *x*, *y*, and *z* with and without high-pass filter (HF). Long-term drift effect have been reduced with use of HF which is clearly shown in the dotted lines.

conducting these initial experiments creates a basic understanding of IMU and its parameters affecting the accuracy of measurements. We developed the orientation detection process through these experiments, reducing the long-term drift and sensitivity issues for distance measurements. Figures 6 and 7 shows different output profiles of velocity and position, respectively of the KPE. Figure 6 compare the velocity components v_x, v_y, and v_z with and without HF. It shows that the slope of v_x, v_y, and v_z decreases with HF which indicates the reduction of long-term drift effect in KPE. Figure 7 illustrates the position components *x*, *y*, and *z* variation with respect to the time with and without HF. We observed that the long-term drift effect has been reduced with use of HF which is clearly presented with dotted lines. In Figs. 6 and 7 the values at t=0 is not zero, which may look like zero-drift error. However, prior to commencing the measurements, we calibrated the sensor to eliminate any potential zero-drift. The results in Figures 6 and 7 present a 20s sample of the data. The values observed at t=0 reflect the initial velocity and position at the onset of the experiment, rather than any zero-drift error. Thus, the observed behaviour in the graphs is a representation of the initial conditions and the high-pass filtering process, and not an artifact of zero-drift.

Using the earth frame acceleration, we performed the course correction of the location whenever there is a loss of GPS signal. When the GPS signal is available KPE update the actual location, however when there is no GPS signal the KPE impose the Kalman filter prediction algorithm as describe in (12),

$$\begin{bmatrix} p \\ v \end{bmatrix} = \begin{bmatrix} 1 & \Delta t \\ 0 & 1 \end{bmatrix} \times \begin{bmatrix} p \\ v \end{bmatrix}_{PreviousState} + \begin{bmatrix} \frac{1}{2} \cdot \Delta t^2 \\ \Delta t \end{bmatrix} \times a \qquad (12)$$

Here p represents the position, and velocity is defined as v. The Earth frame acceleration is denoted as a. Here the previous state is basically the previous known position and velocity. Δt is the time difference. IMU and GPS fused coordinates are depicted with dot (green) symbols in Fig. 8.

Fig. 8. IMU and GPS fused coordinates are depicted with dot (green) symbols. Solid line (light blue) indicates the estimated path obtained from KPE.

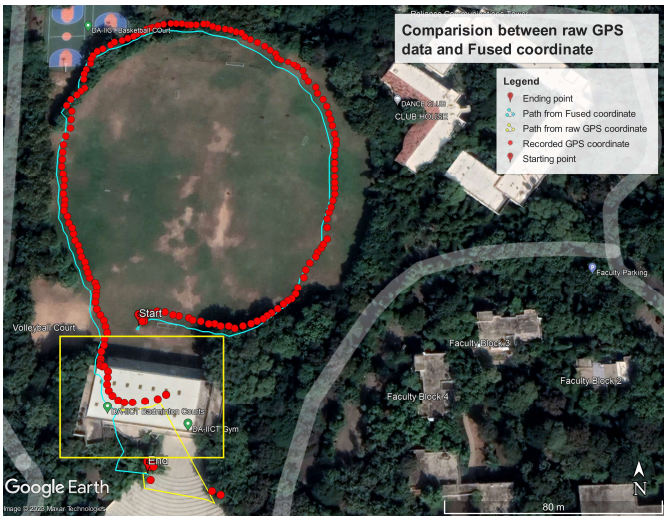

Fig. 9. Comparison of measured GPS data (depicted earlier in Fig. 4) and estimated path obtained using KPE. The yellow square box highlighted that the missing of few red points measured from GPS which results inaccurate response of GPS for indoor navigation. This inaccuracy is solved with the help of fused IMU and GPS responses.

Solid line (light blue) indicates the estimated path obtained from KPE. In the Fig. 9 we observed that the path formed by GPS measured data and our proposed GPS IMU integrated system data remain same in the outdoor environment as there is no GPS outrageous. Whereas when we enter into the indoor environment the GPS sensor losses its ability to connect to the satellite due to thick wall. Hence, we observed a discontinuity in the GPS measured data. In this scenario the IMU sensor takes the control, we have seen that the output of our proposed algorithm closely follows the actual path of travel through the indoor environment. In the indoor environment when the GPS signal is not available it gives the error values which is around 20*m* deviated from the actual position whereas the fusion algorithm gives the output value with less than 1 *m* error.

IV. Evaluation of Kinematic Parameters Estimator

For global position, we used a GPS sensor which gives the KPE longitude, latitude and altitude after connecting with the

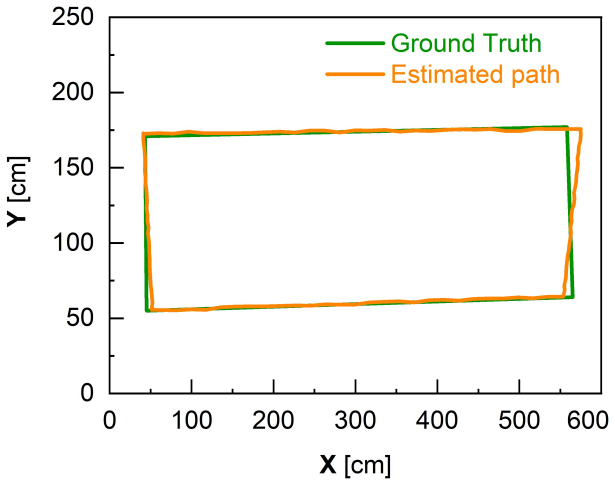

Fig. 10. Comparison of distance measurements using only IMU sensor with respect to the ground truth value. The blue line indicates the ground truth value of the path travelled and the red line shows the path determined by the IMU sensors.

GNSS satellite. Our initial experiments with GPS sensor show us that although GPS accurately measures position in outdoor clear sky conditions in indoor applications, it becomes almost useless as it does not get any GPS signal inside any thick wall or ceiling. Figure 4 shows the coordinator recorded during movement in an open ground including indoor environment. The GPS readings are accurate in the open ground but in case of the indoor environment we noticed some sudden jump in the coordinate (see Fig. 9 highlighted with yellow box). The main reason for this is that GPS signals are transmitted at a frequency of around 1.5 GHz, which may be obstructed or weakened by physical barriers such as thick walls, ceilings, tall buildings, and other structures. This can result in reduced accuracy or complete loss of GPS signal indoors or in areas with poor satellite visibility. The reason for this discontinuous GPS signal in indoor area is because GPS signals work by line-of-sight communication, meaning that the receiver needs to have a direct view of the GPS satellites in the sky to receive accurate position information. When obstacles block the direct path between the GPS receiver and the satellites, the signal can be reflected, refracted, or absorbed by the obstacles, leading to signal degradation or loss.

Conversely, within an indoor environment, IMU sensors exhibit good accuracy in determining relative position, specifically distance traveled on a two-dimensional plane. We conducted several experimental tests to determine the average error in our calculations. We traced an approximately rectangular path and, through comparison, evaluated the accuracy. Figure 10 illustrates experimental data acquired solely from the IMU sensor, compared to a ground truth reference path. However, this functionality is limited to short ranges, typically within a few meters. Additionally, IMU sensors are not suited for absolute coordinate determination (e.g., mapping with GPS readings). Notably, the drift and sensor noise introduce significant errors during long-range distance measurements. Therefore, IMUs alone are incapable of establishing a device's global position and are not recommended for long-distance applications.

We fused the GPS and IMU sensors for position estimation

Fig. 11. Comparison of GPS IMU fusion data with the ground truth value. The green dotted line shows the IMU GPS fusion data and the blue line indicates the ground truth value.

TABLE I
COMPARES ALGORITHMS IN TERMS OF THEIR ACCURACY

Algorithm	IMU	GPS	IMU + GPS
Extended Kalman Filter (EKF) [18]	0.44m (/100m)	--	--
Sensor Fusion on IMU [19]	0.25m (/40m)	--	--
IMU and UWB sensor fusion with EKF [20]	0.2m (/50m)	--	--
Particle filter [21]	1.26m (/150m)	--	--
Tightly coupled integration of Precise Point Positioning (PPP) with Reduced Inertial Sensor System (RISS) [15]	--	--	0.2m (/500m)
Tightly coupled integration of PPP with MEMS-IMU [17]	--	--	1.68m (/20km)
DGPS/MEMS-IMU multi-receiver fusion Motion Capture (MOCAP) system [29]	--	--	0.0394m
This work	0.04m (0.3m)	20m indoor	< 1m indoor + outdoor

to mitigate these challenges. This results an accurate position from GPS when it is connected to the satellite, and IMU assists the positioning system during GPS signal attenuation. Once the GPS signal got restored, it does the course correction for the position determined by the IMU. In this way, the system handled the GPS outages and also reduce the error associated with the IMU measurements. This gives a stable and highly accurate position in the form of the global coordinate (latitude, longitude). Validating experimental data in GPS-denied environments presents a significant challenge, as none of the devices used in our study were capable of recording actual ground truth data under such conditions. This limitation renders direct comparison between experimental results and ground truth data infeasible. To address this, we manually established ground truth values in specific scenarios. For instance, we selected a straight road with an underpass, measuring over 500m in total length, with the underpass itself extending approximately 160m. Despite the lack of GPS signals within the underpass, our device demonstrated a high accuracy in approximating the path when compared to the manually established ground truth. The device achieves an error of less than 1 meter. In our visual representations in Fig. 11, the ground truth path is indicated by a blue line, and the

underpass area is highlighted in red. The comparison in position accuracy of existing literatures with our proposed method is summarized in Table I. It shows that the research results published for individual sort-range or long-range solution. However, our proposed method demonstrates that the KPE can be used for the both case with higher accuracy.

V. Conclusions

In this study, we developed a kinematic parameters estimator (KPE) for both indoor and outdoor positioning by integrating data from IMU and GPS sensors using a Kalman filter. This fusion enables accurate short-range and long-range position estimation. Experimental validations in various environments have demonstrated the effectiveness of the proposed KPE. Our system effectively addresses the challenges posed by individual positioning methods. By fusing GPS and IMU data, it mitigates the impact of GPS outages and reduces the errors inherent in IMU measurements, ensuring stable and highly accurate positioning in global coordinates (latitude and longitude). The KPE operates efficiently in real-time and maintains precise location detection even in GPS-denied environments such as underpasses, tunnels, urban canyons, underground settings, and dense forests.

Specifically, we achieved a short-range position accuracy of approximately 0.04m using only the IMU. For indoor environments, GPS alone provided an accuracy of around 20m, while the KPE achieved an accuracy of less than 1m in both indoor and outdoor settings. These results highlight that while GPS delivers highly accurate location information in outdoor environments, its performance significantly degrades indoors due to signal attenuation and reflection. In contrast, the IMU's contribution becomes critical in indoor environments, providing essential data for the KPE's position and orientation estimates when GPS signals are unreliable. The performance of the KPE has been rigorously verified through multiple field trials, demonstrating centimeter-level accuracy for short-range positioning in the local frame and meter-level accuracy for long-range positioning in global coordinates. This robust performance highlights the potential of the KPE to enhance positioning accuracy in diverse and challenging environments.

References

[1] H. Zhao, C. Wen, S. Zhou, and Y.-H. Liu, "Parameter Estimation of an Industrial Car-Like Tractor," *IEEE Robot. Automat. Lett.*, vol. 6, no. 3, pp.4480 - 4487, Jul. 2021, doi: 10.1109/LRA.2021.3068943.

[2] S. Y. Song, Y. Pei and E. T. Hsiao-Wecksler, "Estimating Relative Angles Using Two Inertial Measurement Units Without Magnetometers," *IEEE Sensors Journal*, vol. 22, no. 20, pp. 19688-19699, 15 Oct.15, 2022, doi: 10.1109/JSEN.2022.3203346.

[3] R. Parween, M. Vega Heredia, M. M. Rayguru, R. Enjikalayil Abdulkader, and M. R. Elara, "Autonomous Self-Reconfigurable Floor Cleaning Robot," *IEEE Access*, vol. 8, pp. 114433-114442, 2020, doi: 10.1109/ACCESS.2020.2999202.

[4] M. Vigne, A. El Khoury, F. Di Meglio and N. Petit, "State Estimation for a Legged Robot With Multiple Flexibilities Using IMUs: A Kinematic Approach," *IEEE Robot. Automat. Lett.*, vol. 5, no. 1, pp. 195-202, Jan. 2020, doi: 10.1109/LRA.2019.2953006.

[5] A. Baghdadi, L. A. Cavuoto and J. L. Crassidis, "Hip and Trunk Kinematics Estimation in Gait Through Kalman Filter Using IMU Data at the Ankle," *IEEE Sensors Journal*, vol. 18, no. 10, pp. 4253-4260, 15 May 2018, doi: 10.1109/JSEN.2018.2817228.

[6] J. Wahlström, I. Skog, P. Händel and A. Nehorai, "IMU-Based Smartphone-to-Vehicle Positioning," *IEEE Trans. Intel. Vehicle.*, vol. 1, no. 2, pp. 139-147, June 2016, doi: 10.1109/TIV.2016.2588978.

[7] H. Yang et al., "Smartphone-Based Indoor Localization System Using Inertial Sensor and Acoustic Transmitter/Receiver," *IEEE Sensors Journal*, vol. 16, no. 22, pp. 8051-8061, Nov., 2016, doi: 10.1109/JSEN.2016.2604424.

[8] A. R. J. Jiménez Ruiz, F. Seco Granja, J. Carlos Prieto Honorato and J. I. Guevara Rosas, "Pedestrian indoor navigation by aiding a foot-mounted IMU with RFID Signal Strength measurements," *Int. Conf. Indoor Pos. and Indoor Nav.*, pp.1-7, 2010, Zurich, Switzerland, 2010, doi: 10.1109/IPIN.2010.5646885.

[9] C. Ascher, L. Zwirello, T. Zwick and G. Trommer, "Integrity monitoring for UWB/INS tightly coupled pedestrian indoor scenarios," *Int. Conf. Indoor Pos and Indoor Nav.*, Guimaraes, pp.1-6, 211, Portugal, doi: 10.1109/IPIN.2011.6071948.

[10] H. Zhang and C. Ye, "Plane-Aided Visual-Inertial Odometry for 6-DOF Pose Estimation of a Robotic Navigation Aid," *IEEE Access*, vol. 8, pp. 90042-90051, 2020, doi: 10.1109/ACCESS.2020.2994299.

[11] W. Lee, P. Geneva, Y. Yang and G. Huang, "Tightly-coupled GNSS-aided Visual-Inertial Localization," *Int. Conf. Robotic. Auto. (ICRA)*, pp. 9484-9491, 2022, Philadelphia, PA, USA, doi: 10.1109/ICRA46639.2022.9811362.

[12] D. B. Ahmed and E. M. Diaz, "3D Loose-Coupled Fusion of Inertial Sensors for Pedestrian Localization," *Int. Conf. Indoor Pos. Indoor Navig. (IPIN)*, pp. 206-212, 2018, Nantes, France, doi: 10.1109/IPIN.2018.8533795.

[13] D. R. -Y. Phang, W. -K. Lee, N. Matsuhira and P. Michail, "Enhanced Mobile Robot Localization with Lidar and IMU Sensor," *IEEE Int. Meet. Future Electron Dev., Kansai (IMFEDK*), Kyoto, Japan, 2019, pp. 71-72, doi: 10.1109/IMFEDK48381.2019.8950726.

[14] S. Dutta, T. K. Maiti, M. Miura-Mattausch, Y. Ochi, N. Yorino, and H. J. Mattausch, "Analysis of Sensor-Based Real-Time Balancing of Humanoid Robots on Inclined Surfaces," *IEEE Access*, pp.212327-212338, vol. 8, Nov 2020, doi: 10.1109/ACCESS.2020.3040001.

[15] M. Elsheikh, A. Noureldin and M. Korenberg, "Integration of GNSS Precise Point Positioning and Reduced Inertial Sensor System for Lane-Level Car Navigation," *IEEE Trans. Intel. Transport. System*, vol. 23, no. 3, pp. 2246-2261, March 2022, doi: 10.1109/TITS.2020.3040955.

[16] A. Toda and Y. Koike, "Simulation Design of Thermopile and Magnetometer Aided INS/GPS Navigation System for UAV Navigation," *IEEE Int. Symp. Inertial Sensors and Systems (INERTIAL)*, pp. 1-4, 2021, Kailua-Kona, HI, USA, doi: 10.1109/INERTIAL51137.2021.9430487.

[17] M. Abd Rabbou and A. El-Rabbany, "Tightly coupled integration of GPS precise point positioning and MEMS-based inertial systems," *GPS Solutions*, vol. 19, no. 4, pp. 601–609, Oct. 2014, doi: 10.1007/s10291-014-0415-3.

[18] H. Hellmers, A. Norrdine, J. Blankenbach and A. Eichhorn, "An IMU/magnetometer-based Indoor positioning system using Kalman filtering," *Int. Conf. Indoor Pos. Indoor Nav.*, pp. 1-9, 2013, Montbeliard, France, doi: 10.1109/IPIN.2013.6817887.

[19] A. Poulose, O. S. Eyobu, and D. S. Han, "An Indoor Position-Estimation Algorithm Using Smartphone IMU Sensor Data," *IEEE Access*, vol. 7, pp. 11165–11177, 2019, 2019, doi: 10.1109/ACCESS.2019.2891942.

[20] L. Yao, Y. -W. A. Wu, L. Yao and Z. Z. Liao, "An integrated IMU and UWB sensor based indoor positioning system," *Int. Conf. Indoor Pos. Indoor Nav. (IPIN)*, pp. 1-8, 2017, Sapporo, Japan, doi: 10.1109/IPIN.2017.8115911.

[21] Y. Liu, M. Dashti, M. A. Abd Rahman and J. Zhang, "Indoor localization using smartphone inertial sensors," *Workshop on Positioning, Navigation and Communication (WPNC)*, pp. 1-6, 2014, Dresden, Germany, doi: 10.1109/WPNC.2014.6843288.

[22] I. G. Fernandez, C. Wada and S. A. Ahmad, "Walking Cane Velocity Estimation using a Velocity Update Method," *IEEE 3rd Global Conference on Life Sciences and Technologies (LifeTech)*, pp. 249-252, 2021, Nara, Japan, doi: 10.1109/LifeTech52111.2021.9391813.

[23] BNO055: https://cdn-shop.adafruit.com/datasheets/BST_BNO055_DS000_12.pdf

[24] MTK3339: https://cdn-shop.adafruit.com/product-files/746/CD+PA1616S+Datasheet.v03.pdf

[25] ATmega328: https://www.microchip.com/en-us/product/atmega328

[26] R. E. Kalman, “A New Approach to Linear Filtering and Prediction Problems,” *J. Basic Eng*., vol. 82, no. 1, pp. 35–45, Mar. 1960, doi: 10.1115/1.3662552.
[27] S. O. H. Madgwick, A. J. L. Harrison and R. Vaidyanathan, “Estimation of IMU and MARG orientation using a gradient descent algorithm,” *IEEE Int. Conf. on Rehab. Robot.*, pp.1-7, 2011, Zurich, Switzerland, doi: 10.1109/ICORR.2011.5975346.
[28] G. Fastellini, F. Radicioni, A. Schiavoni, and A. Stoppini, “Comparison of kinematic parameters of a moving vehicle by GNSS measurements and inertial/GPS navigation system,” *the 5th International Symposium on Mobile Mapping Technology (MMT), Padua, Italy*, pp. 29–31, 2007. https://www.isprs.org/proceedings/XXXVI/5-C55/papers/radicioni_fabio_1.pdf
[29] D. Y. Ku, “Kinematic State Estimation using Multiple DGPS/MEMS-IMU Sensors," MS thesis, Department of Electrical Engineering, University of Cape Town, South Africa, 2020. http://hdl.handle.net/11427/36851
[30] D. Y. Ku and A. Patel, "Kinematic State Estimation Using Multiple DGPS/MEMS-IMU Sensors," *IEEE Sensors Letters*, vol. 4, no. 12, pp. 1-4, Dec. 2020, doi: 10.1109/LSENS.2020.3040661.
[31] L. Zhang, H. Zhao, J. Chen, L. Li, and X. Liu, ‘Vehicular positioning based on GPS/IMU data fusion aided by V2X networks’, *IEEE Sensors Journal*, vol. 24, no. 6, pp. 9032-9043, 15 March15, 2024, doi: 10.1109/JSEN.2024.3355185.
[32] H. Zhang, H. Xiong, S. Hao, G. Yang, M. Wang and Q. Chen, "A Novel Multidimensional Hybrid Position Compensation Method for INS/GPS Integrated Navigation Systems During GPS Outages," *IEEE Sensors Journal*, vol. 24, no. 1, pp. 962-974, 1 Jan.1, 2024, doi: 10.1109/JSEN.2023.3324019.
[33] M. Zhang, Y. Luo, and K. A. Neusypin, ‘Research on Combined GNSS/IMU/Camera Positioning and Navigation in Full Scene’, in *2024 International Russian Smart Industry Conference (SmartIndustryCon)*, Sochi, Russian Federation, pp. 327-332, 2024, doi: 10.1109/SmartIndustryCon61328.2024.10516097.
[34] Y. H. Park, M. G. Kang, J. H. Jeong, and S. G. Choi, ‘The Data Alignment Method Between GPS and IMU Based on ICP for Indoor Positioning’, in *2024 26th International Conference on Advanced Communications Technology (ICACT)*, Pyeong Chang, Korea, Republic of, pp. 369-372, 2024, doi: 10.23919/ICACT60172.2024.10471932.

S. Paul received B.Sc. degree in physics from Vidyasagar University, WB, India in 2020. He also obtained M.Sc. degree in Electronics with a Gold Medal in 2022 from Vidyasagar University, WB. India and a Gold Medal from Sitaram Jindal Foundation.

He worked as a JRF in a GUJCOST funded Robotics project at Dhirubhai Ambani Institute of Information and Communication Technology, Gandhinagar, Gujarat.

T. K. Maiti (M’16) received the Ph.D. degree in Engineering from Jadavpur University, Kolkata, India, in 2009.

He has held various positions at Hiroshima University, Japan, McMaster University, Canada, IIT-Kharagpur and IIEST-Shibpur, India. Since 2019, he has been Associate Professor with DA-IICT, Gandhinagar, India, where he is involved in research on Intelligent Circuits and Systems, Robotics, and Cybernetics.